Single-Photon Tunneling via Localized Surface Plasmons

I. I. Smolyaninov,[1] A. V. Zayats,[2] A. Gungor,[3] and C. C. Davis[1]

[1]*Electrical and Computer Engineering Department, University of Maryland, College Park, Maryland 20742*
[2]*Department of Pure and Applied Physics, Queen's University of Belfast, Belfast BT7 1NN, United Kingdom*
[3]*Department of Physics, Fatih University, Istanbul, Turkey*

(Received 5 October 2001; published 23 April 2002)

Strong evidence of a single-photon tunneling effect, a direct analog of single-electron tunneling, has been obtained in the measurements of light tunneling through individual subwavelength pinholes in a gold film covered with a layer of polydiacetylene. The transmission of some pinholes reached saturation because of the optical nonlinearity of polydiacetylene at a very low light intensity of a few thousand photons per second. This result is explained theoretically in terms of a "photon blockade," similar to the Coulomb blockade phenomenon observed in single-electron tunneling experiments. Single-photon tunneling may find applications in the fields of quantum communication and information processing.

DOI: 10.1103/PhysRevLett.88.187402 PACS numbers: 78.67.–n, 42.50.–p, 42.65.–k

The emerging fields of quantum communication and information processing require unusual sources of light with strong quantum correlations between single photons, and new types of light detectors that can detect individual photons without destroying them [1]. A few such novel quantum devices have been demonstrated very recently, such as a quantum dot single-photon turnstile device, and a quantum nondemolition photon detector based on strong photon-matter coupling [2,3]. Operation of such quantum devices is extremely involved, and there is a great need for novel ideas and device concepts in this field. One such idea is the concept of photon blockade in a nonlinear optical cavity [4], introduced theoretically in close analogy with the well-known phenomenon of Coulomb blockade for quantum-well electrons. The suggested realization of this concept involves a four-level atomic system in a macroscopic optical cavity, which exhibits resonantly enhanced two-photon absorption limited Kerr nonlinearity. The optical transmission of such a cavity is supposed to exhibit photon antibunching.

In this Letter we suggest and demonstrate experimentally a new example of photon blockade, which is based on close analogy between electron and photon tunneling. It is well known that Coulomb blockade leads to the observation of single-electron tunneling in tunnel junctions with an extremely small capacitance, where the charging energy $e^2/2C$ of the capacitance C is much larger than the thermal energy k_BT and the quantum fluctuation energy $\hbar/RC$ where R is the resistance of the tunnel junction [5,6]. An example of such a tunnel junction is shown in Fig. 1(a), where a nanoparticle with a very small capacitance C is placed in the gap between the tip and sample of a scanning tunneling microscope (STM). In this case, tunneling of a single electron into the nanoparticle results in noticeable charging of the junction capacitance, so the probability of other tunneling events is drastically reduced. Therefore, there is a strong correlation between tunneling events [5,6]: electrons tunnel one at a time, and steps ("Coulomb staircase") in the current-voltage characteristic of a tunnel junction are observed.

Let us consider a geometry of an optical single-photon tunneling experiment [Fig. 2(b)] designed to emulate the geometry of a single-electron tunneling experiment. Classical realization of light tunneling is based on a glass surface illuminated in the total internal reflection geometry, e.g., using a prism or a semicylinder. In this case, all incident light is reflected and only an evanescent field (exponentially decaying from the surface) exists over a smooth surface. If a tapered glass fiber is placed sufficiently close to the glass-air interface, the evanescent field is transformed into propagating waves in the fiber. Thus, optical tunneling through an air gap (which can be considered as a tunnel barrier) occurs. This geometry is used in a scanning tunneling optical microscope (STOM) operation.

To complete our analogy to single-electron tunneling, we will consider a nanometer-scale object in the tunnel gap of a STOM. Let us assume that this object possesses nonlinear optical properties and exhibits well defined localized electromagnetic modes. There are quite a few examples of such objects. It may be a silver-coated polymerized

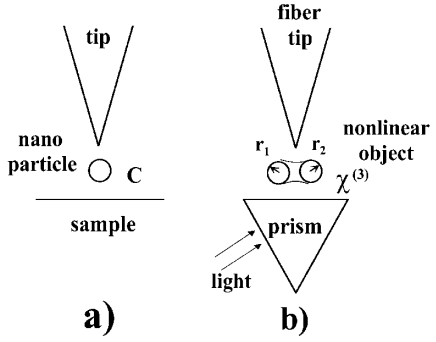

FIG. 1. Schematic views of single-electron (a) and single-photon (b) tunneling experiments. The nonlinear object in (b) is represented by two metallic nanoparticles with radii r_1 and r_2 separated by a gap filled with nonlinear optical material.

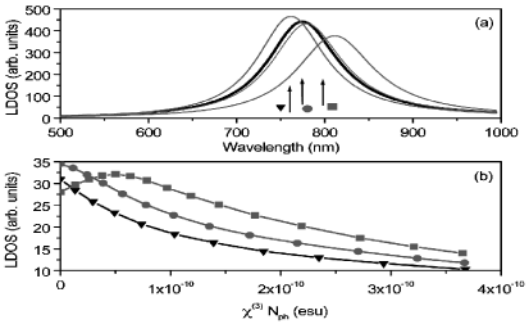

FIG. 2. LDOS spectra (a) and intensity dependencies (b) of LDOS at the wavelengths indicated by arrows calculated for the 10 nm spherical silver particle placed at a 1 nm distance from a second silver particle with a much larger diameter. The gap between the particles is filled with a nonlinear material. The LDOS spectra correspond to different changes of the refractive index of a nonlinear material: (from left to right) $\Delta n = -0.03$, 0, 0.01, and 0.1. The linear refractive index of the nonlinear material ($n_0 = 1.7$) is chosen close to the refractive index of BCMU polydiacetylene.

diacetylene composite nanoparticle [7], or a narrow gap between two silver or gold nanoparticles with radii r_1 and r_2 filled with nonlinear optical material as shown in Fig. 1(b). Nanometer-size gaps between metal surfaces (such as a tip and a sample of an STM) are known to exhibit pronounced and well-defined localized surface plasmon (LSP) resonances [8,9]. Excitation of LSP modes may lead to very large local electromagnetic field intensity enhancement [10] because of the very small volume of these modes. If the frequency of tunneling photons is in resonance with some localized optical mode of the nanometer-scale object in Fig. 1(b), tunneling from the sample into the tip of the STOM is facilitated. This happens via excitation of the localized mode. The electric field of the excited localized mode E_L induces local changes in the dielectric constant ϵ of the nonlinear optical material:

$$\epsilon = \epsilon^{(1)} + 4\pi\chi^{(3)}|E_L|^2, \tag{1}$$

where $\epsilon^{(1)}$ and $\chi^{(3)}$ are the linear dielectric constant and the third-order nonlinear susceptibility, respectively (here we consider the case of a central symmetric nonlinear material with $\chi^{(2)} = 0$). As a consequence of dielectric constant change, the localized modes may experience a noticeable frequency change, so that the tunneling photons will not be in resonance any more. Thus, photon tunneling will be blocked in a manner similar to the Coulomb blockade effect for electrons in Fig. 1(a), until the localized optical mode has radiated and the nonlinear material relaxes into its initial state. Our calculations below indicate that in some cases even tunneling of a single optical quantum into the localized plasmon mode is enough to cause an effective blockade of the tunneling gap for the next optical quanta. In this analogy between Coulomb and photon blockade, illuminating light intensity plays a role similar to the role of tunneling voltage in single-electron tunneling experiments. Similar to the effect of bias voltage, the larger illuminating light intensity, the more localized optical modes become available for the transmission, resulting in the staircase behavior similar to the Coulomb staircase. If the position of the localized optical modes can be shifted by some external perturbation, for example, by external stress provided by a piezo actuator (localized plasmon modes are strongly size dependent), this external perturbation will play a role similar to the role of the gate voltage in single-electron tunneling devices [11], where the gate voltage is used to tune the transmission between different states. One can also expect some similarity in the effect of temperature on both phenomena. If k_BT is of the order of $\hbar\omega$ for localized plasmon modes, single-photon tunneling could not be observed because of thermal excitation of these modes. Temperature effect may be a problem for measurements in the infrared range.

Unless we are interested in the space-time dynamics of photon tunneling, a formal analogy between electron and photon tunneling can be drawn [12]. In the widely used theory of STM [13] the tunneling current is proportional to the local density of states (LDOS) of a sample under investigation, $\rho_s(\mathbf{r}, E_F)$, at the Fermi energy:

$$I \sim \rho_s(\mathbf{r}, E_F). \tag{2}$$

Single-electron tunneling can be realized in systems in which tunneling electrons (ultimately, one electron) significantly modify the energy spectrum of LDOS $\rho_s(\mathbf{r}, E_F)$ by, for example, influencing the Fermi energy of the sample [the nanoparticle in Fig. 1(a)].

The LDOS for photons (sometimes referred to as the photonic mode density) can be defined in the same way as is done for electrons via the electric field dyadic Green function $\mathbf{G}(\mathbf{r}, \mathbf{r}', \omega)$ of a system under consideration [14]:

$$\rho(\mathbf{r}, \hbar\omega) = -1/\pi\, \mathrm{Im}\mathbf{G}(\mathbf{r}, \mathbf{r}, \hbar\omega), \tag{3}$$

which gives the density of states of electromagnetic eigenmodes of energy $\hbar\omega$. The physical interpretation of the LDOS in optics is that it is directly related to the square of the modulus of the electric field at a given point in space $\mathbf{r}$ and at a given photon energy $\hbar\omega$, and, therefore, to the electromagnetic field enhancement in the system.

Similar to single-electron tunneling, which is observed in systems in which tunneling electrons significantly modify the energy spectrum of LDOS, tunneling photons can significantly modify the LDOS spectrum of a system exhibiting third-order nonlinear effects through local changes of the dielectric constant. As a consequence of the refractive index change, the polarizability and, therefore, the LDOS of the system are modified. A nonabsorbing electro-optical nonlinearity should be employed to avoid optical losses in a nonlinear material. For a particle made of dielectric material with a low dispersion refractive index, the LDOS has a broad continuous spectrum, thus requiring significant intensities of the incoming light for controlling the particle polarizability. In contrast, small metallic particles made of gold or silver exhibit a narrow-band LDOS spectrum in the spectral range where localized surface plasmons are excited. In the maximum of the band, a

significant enhancement of the electromagnetic field occurs in the vicinity of the particle in turn enhancing the nonlinear effects. Thus, realization of light controlled photon tunneling can be achieved combining high third-order nonlinear materials with good metals exhibiting a narrow spectrum of LDOS and strong field enhancement effects.

A very strong field enhancement is expected in the narrow gap between two silver or gold nanoparticles when the electromagnetic near-field interaction modifies significantly the plasma resonances of the nanoparticles, resulting in the surface plasmon's localization in the gap between the particles. As the highest field enhancement is expected in this system, in general, for small nanoparticle separations d, we shall consider the situation $d \ll r_1 = R \ll r_2$ that simplifies the LDOS spectrum calculation significantly [8,9]. This model has been successfully employed for describing the surface enhanced Raman scattering, photon emission from STM, etc. In our case we assume that the gap d between the metallic particles is filled with a nonlinear material. The LDOS spectrum of such a system can be calculated analytically in the limit $d \ll R$ since it formally resembles particle motion in the Coulomb field [15], and is determined by the following dispersion relation [8]:

$$\mathrm{Re}[\epsilon/\epsilon(\omega)] = -(m + 1/2)\,(d/2R)^{1/2}, \quad m = 0, 1, 2 \ldots, \tag{4}$$

where ϵ and $\epsilon(\omega)$ are the dielectric constants of nonlinear material and metal, respectively, R is the radius of the smaller nanoparticle, and d is the gap between the particles. The quantum number m corresponds to different localized surface plasmon modes in the gap. The strongest localization occurs for the lowest, $m = 0$, mode with a localization length $L = (2dR)^{1/2}$, and the electric field of this localized mode is determined by the potential

$$\phi(k) = A\frac{\exp(-kL)}{k\epsilon}, \tag{5}$$

where A is the normalization constant. Having determined the mode volume of this localized plasmon, the respective electric field in the gap can be calculated and the related electro-optical nonlinearity estimated [Eq. (1)] for a given number of tunneling photons [16]. The results of our calculations are shown in Fig. 2. The LDOS in the gap is presented as a function of light wavelength [Fig. 2(a)] for different values of the nonlinear refractive index change caused by excitation of a localized plasmon mode. Figure 2(b) shows the changes in the LDOS at different light intensities (different numbers of plasmon quanta excited in the gap) for the incident light wavelength corresponding to the LSP resonance at low light intensities, as well as for the longer and shorter wavelengths. With an increase of the incident light intensity the LDOS resonance shift leads to significant variations of LDOS at the illumination wavelength. The decrease of the LDOS results in the saturation of transmitted light intensity with an increase of the incident light intensity. Because of very strong field localization, the number of photons required to achieve a "photon blockade" is very low. If $\chi^{(3)} \sim 10^{-10}$ esu is assumed, which is on the correct order of magnitude for the $\chi^{(3)}$ observed in poly-3-butoxy-carbonyl-methyl-urethane (3BCMU) and 4BCMU polydiacetylene materials [17] (these central symmetric materials with $\chi^{(2)} = 0$ hold the record for the largest fast nonresonant optical $\chi^{(3)}$ nonlinearity), there is a fair chance to observe single-photon tunneling, since a single tunneled photon causes the reduction of LDOS at the incident light wavelength by almost a factor of 2.

The measurements of light tunneling through individual subwavelength pinholes in a thick gold film covered with a layer of polydiacetylene provide strong evidence of single-photon tunneling. Our experimental setup is shown in Fig. 3. A thick ($\sim$0.5 μm) gold film had been thermally deposited on the surface of a glass prism. Microscopic images of the film revealed the usual granular structure of the film with the size of individual grains in the 10–100 nm range. Only a few sparsely separated pinholes were visible in the film under illumination with 632 nm light at an angle larger than the angle of total internal reflection for the glass-air interface. Since the pinholes are located at the grain boundaries, the theoretical model described above provides a reasonable description of the optical properties of gaps (if any) between the grains in the film. A drop of 3BCMU polydiacetylene solution in chloroform [18] was deposited onto the gold film surface. After solvent evaporation a thick film of polydiacetylene was left on the surface. A cleaved optical fiber with a core diameter of about 9 μm was used to collect 632 nm light transmitted through the individual pinholes. The fiber was positioned above individual pinholes at a distance of a few micrometers using a far-field optical microscope and the shear-force distance control system commonly used in near-field optical setups [19]. The pinholes selected for the measurements had very low optical transmission of a few hundred photons per second. An additional advantage of this experimental geometry with respect to the idealized situation shown in Fig. 1(b) is the absence of any background scattered light which could be collected by the fiber. Figure 4 shows the measured dependencies of the transmitted light as a function of the illuminated light intensity for some selected pinholes. The size a of these pinholes may be roughly

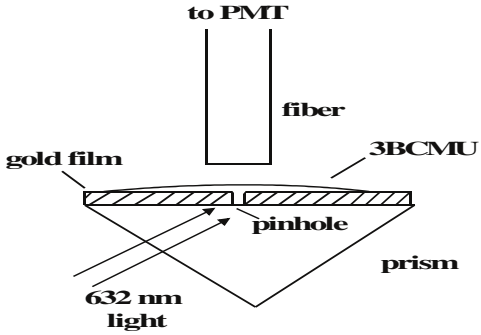

FIG. 3. Schematic view of our experimental setup.

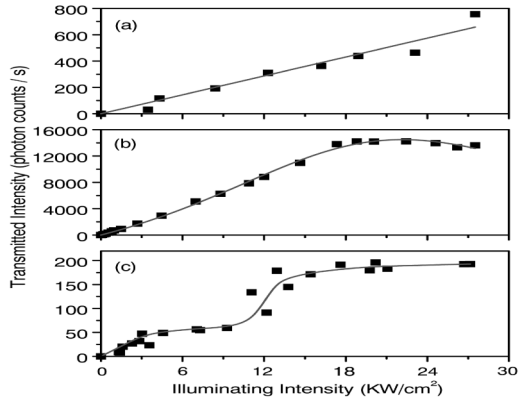

FIG. 4. Experimentally measured transmission of three different subwavelength pinholes at $\lambda = 632$ nm. Saturation of transmission due to the optical nonlinearity of polydiacetylene at a very low light intensity of a few thousand photons per second has been observed in (b) and (c). Solid lines are the fits in the model of the intensity dependent LDOS resonances.

estimated using the Bethe's expression for the cross section of a subwavelength aperture [20]: $A \sim a^2(a/\lambda)^4$. Using the numerical data from Fig. 4(a) we have an estimate of $a \sim 7$ nm, which corresponds to a desired range of pinhole sizes. While the dependencies obtained for most pinholes were linear, transmission of some small pinholes exhibited saturation and even staircaselike behavior.

The experimental data has been fitted assuming the intensity dependent LDOS resonances analogous to the model described above. The LSP spectral positions have been used as fitting parameters. Although the absolute spectral positions of the resonances related to nanopores can be somewhat different from the ones given by Eq. (4), a similar dependence on light intensity has been assumed for fitting. The fitting curves obtained with one [Fig. 4(b) and two [Fig. 4(c)] intensity dependent local plasmon resonances show good agreement with the experiment. For a two-resonance curve [Fig. 4(c)], the second resonance observed at higher light intensity is presumed to be initially far away from the frequency of the incident light [cf. Fig. 2(a)]. It becomes significant only at higher intensities at which lower resonance is almost constantly excited contributing to the nonlinear refractive index change and thus to the spectral shift of the higher resonance with light intensity. Thus, at low illuminating light intensity, photons tunnel via the excitation of the nearest localized surface plasmon. With the increase of the intensity, the excitation rate of the second nearest LSP increases and it begins to contribute to the tunneling, leading to the second step in the transmittance curve [Fig. 4(c)]. Excitation of the second resonance in turn leads to the additional refractive index change resulting in the saturation of this second tunneling channel. This interplay between the resonances leads to the staircaselike behavior of the observed transmission.

Unlike the case of Coulomb blockade, where at $e^2/2C \gg k_BT$ there is no transmission until a certain voltage is achieved, all the experimental curves shown in Fig. 4 exhibit linear growth at small light intensities. We believe that there are two main reasons for this difference. The wavelength of light is much larger than the wavelength of electrons, so unlike single-electron tunneling experiments in the geometry similar to Fig. 1(a), there is a nonzero probability for photons to nonresonantly tunnel directly into the collecting fiber in Fig. 3. On the other hand, the localized plasmon resonances of metal nanoparticles have rather large linewidth. Thus, the staircase transmission behavior should be much less pronounced compared to the Coulomb staircase at low temperatures. Another difference between the Coulomb and photon blockade is due to the fact that unlike electric charge, the number of photons is not conserved: the dominant decay mechanism of localized plasmons in metallic nanoparticles is nonradiative Landau damping [8] where the electromagnetic energy is transferred to electronic excitations. The steps in conductance of a Coulomb blockade device are usually of the order of $2e^2/h$ [11]. Since the current of photons is not conserved, no similar "universal" steps in experimentally measured photon transmission may be expected.

This work was supported in part by the NSF-MRSEC, Grant No. DMR 00-8008.

[1] D. Bouwmeester, A. Ekert, and A. Zeilinger, *The Physics of Quantum Information* (Springer, Berlin, 2000).
[2] P. Michler *et al.,* Science **290**, 2282 (2000).
[3] G. Nogues *et al.,* Nature (London) **400**, 239 (1999).
[4] A. Imamoglu *et al.,* Phys. Rev. Lett. **79**, 1467 (1997).
[5] E. Ben-Jacob and Y. Gefen, Phys. Lett. **108A**, 289 (1985).
[6] D. V. Averin and K. K. Likharev, J. Low Temp. Phys. **62**, 345 (1986).
[7] H. S. Zhou *et al.,* Appl. Phys. Lett. **68**, 1288 (1996).
[8] A. G. Malshukov, Phys. Rep. **194**, 343 (1990).
[9] P. Johanson, R. Monreal, and P. Apell, Phys. Rev. B **42**, 9210 (1990).
[10] V. M. Shalaev, *Nonlinear Optics of Random Media* (Springer, Berlin, 2000).
[11] *Mesoscopic Electron Transport,* edited by L. Sohn *et al.,* NATO ASI, Ser. E, Vol. 345 (Kluwer, Dordrecht, 1997).
[12] R. Y. Chiao and A. M. Steinberg, *Progress in Optics XXXVII,* edited by E. Wolf (North-Holland, Amsterdam, 1995), pp. 345–405.
[13] J. Tersoff and D. R. Hamman, Phys. Rev. B **31**, 805 (1985).
[14] W. L. Barnes, J. Mod. Opt. **45**, 661 (1998).
[15] V. M. Agranovich, V. E. Kravtsov, and T. A. Leskova, Solid State Commun. **47**, 925 (1983).
[16] It is assumed that the Landau damping is the most significant relaxation mechanism in the system. U. Kreibig and M. Vollmer, *Optical Properties of Metal Clusters* (Springer, Berlin, 1995).
[17] K. Yang *et al.,* Opt. Commun. **164**, 203 (1999).
[18] We are grateful to A. Drury and W. Blau, Polymer Research Centre, Trinity College Dublin, for kindly providing the 3BCMU polymer used in the experiment.
[19] E. Betzig, P. L. Finn, and J. S. Weiner, Appl. Phys. Lett. **60**, 2484 (1992).
[20] H. Bethe, Phys. Rev. **66**, 163 (1944).